

OPEN ACCESS

EDITED BY Chenxi Li, Xi'an University of Architecture and Technology, China

REVIEWED BY
Natasha Murtaza,
University of Agriculture, Faisalabad, Pakistan
Qing Wei,
Tongji University, China

*CORRESPONDENCE
Xiaoyan Ma

☑ maxiaoyan@nwafu.edu.cn
Jun Tian
☑ tianjun@xawl.edu.cn

RECEIVED 20 June 2025 ACCEPTED 22 September 2025 PUBLISHED 01 December 2025

CITATION

Chen X, Zhang S, Lin J, Tian J and Ma X (2025) Temporal and spatial evolution of interprovincial CO₂ emissions and driving factors based on a spatial-temporal geo-weighted regression mode. Front. Clim. 7:1649791. doi: 10.3389/fclim.2025.1649791

COPYRIGHT

© 2025 Chen, Zhang, Lin, Tian and Ma. This is an open-access article distributed under the terms of the Creative Commons Attribution License (CC BY). The use, distribution or reproduction in other forums is permitted, provided the original author(s) and the copyright owner(s) are credited and that the original publication in this journal is cited, in accordance with accepted academic practice. No use, distribution or reproduction is permitted which does not comply with these terms.

Temporal and spatial evolution of interprovincial CO₂ emissions and driving factors based on a spatial-temporal geo-weighted regression mode

Xiaolu Chen¹, Shihan Zhang¹, Jiayi Lin², Jun Tian^{1*} and Xiaoyan Ma^{3*}

¹The School of Arts and Design, Xi'an University, Xi'an, China, ²College of Landscape Architecture and Art, Henan Agricultural University, Zhengzhou, China, ³College of Landscape Architecture and Art, Northwest ΑθF University, Yangling, China

Introduction: To support China's "dual carbon" goals (carbon emission peak by 2030 and carbon neutrality by 2060), this study systematically investigates the spatio-temporal evolution and decarbonization pathways of CO₂ emissions across 30 Chinese provinces. As regional disparities significantly influence national climate strategies, a detailed provincial-level analysis is essential for effective policy-making. **Methods:** We integrate spatial autocorrelation analysis, spatio-temporal geographically weighted regression (GTWR/SGTWR), and agglomerative hierarchical clustering with dynamic time warping (DTW-AHC) to capture both spatial and temporal heterogeneities in emission patterns.

Results: The findings reveal that provincial CO_2 emissions exhibit weakening spatial aggregation after 2015, with northern provinces maintaining higher carbon intensity due to heavy reliance on fossil fuels. Energy consumption and transportation collectively account for over 70% of emissions growth after 2008, while emissions from food and water sectors decline after 2016, largely driven by technological advances. Four distinct emission clusters are identified: Rapid Growth, Resource-Dependent, Typical Growth, and Low-Carbon Exemplar.

Discussion: Tailored decarbonization strategies are proposed for each cluster: integrating renewable energy corridors with urban green infrastructure for Rapid Growth provinces; prioritizing ecological restoration and carbon capture, utilization, and storage (CCUS) in Resource-Dependent regions; accelerating green industrial transitions in Typical Growth provinces; and reinforcing existing low-carbon policies for Exemplar provinces. This research provides a spatially explicit framework for regionally differentiated carbon governance, supporting the achievement of China's national climate targets.

KEYWORDS

carbon emission clustering, spatial autocorrelation, dynamic time warping, regional decarbonization, industrial structure

1 Introduction

Anthropogenic carbon dioxide (CO_2) emissions from fossil fuel combustion have been identified as the dominant driver of atmospheric CO_2 concentrations since the Industrial revolution (Zhang and Zhao, 2024). As the world's largest carbon emitter, China plays a pivotal role in global efforts to combat climate change. Given that the industrial sector constitutes a major portion of China's carbon emissions, rigorous analysis of provincial-level industrial emissions becomes

imperative (Wu et al., 2023). In 2020, the Chinese government officially proposed the "double carbon" strategic goals - achieving carbon peaking by 2030 and carbon neutrality by 2060. This commitment entails profound transformations of the energy system and industrial structure optimization (Liang et al., 2024), demonstrating China's international climate responsibility while offering a distinctive sustainable development model.

To advance carbon reduction objectives, scholars predominantly employ spatial econometric methods for qualitative and quantitative investigations (Chen et al., 2018; Meng et al., 2021). These approaches, combined with advanced modeling techniques, reveal spatial agglomeration effects and distribution heterogeneity (Song et al., 2018; Lim et al., 2019) while enabling emissions trajectory projections (Wei and Liu, 2022). For instance, the ESDA-GWR(Exploratory Spatial Data Analysis-Geographically Weighted Regression) methodology was employed to systematically examine the spatial distribution patterns of China's carbon emissions and the spatial heterogeneity of multiple driving factors at the prefecture-level city scale in 2012 (Qin et al., 2019), revealed a pronounced spatial spillover effect predominantly concentrated in eastern regions, where demographic, economic, and industrial factors exerted significantly stronger influences on carbon emissions compared to central and western regions. Similarly, Moran's I and hotspot analyses confirmed positive spatial autocorrelation in shrinking Chinese cities during 2012-2019, with Northeast China emerging as a significant emission hotspot due to concentrated urban contraction (Yang et al., 2022). Complementary research utilizing GWR models established urbanization as the dominant factor in China's annual carbon dioxide emission growth, which indicated that both energy intensity and industrial structure positively influenced carbon emissions, providing valuable insights for emission reduction strategies (Wang et al., 2018). Despite these advances, current research has not systematically elucidated spatial differentiation across emission types or their city-specific response mechanisms.

On the basis of systematically combing the spatial heterogeneity of carbon emissions and its driving factors, it is necessary to further pay attention to the multi-dimensional influence mechanism of human activity pattern changes on carbon emissions in the process of urbanization. Previous research consistently demonstrated the significant impact of human activity patterns on carbon emission growth through complex environmental changes (Liu et al., 2015; Sheng and Guo, 2016). By constructing the urbanization index system including population, public services, infrastructure and environment, the coupling coordination degree of China 's low-carbon development and urbanization system was measured, which showed that the coordination degree of the eastern and western regions was at the highest and lowest levels, respectively, (Song et al., 2018). Spatial autocorrelation analyses of 30 provinces (2010-2019) using a multidimensional urbanization evaluation system further identified a ladder-like spatial gradient in coordination, decreasing from southeastern coastal areas to central and western regions, with significant positive spatial correlation (Jiang et al., 2022). Nevertheless, systematic analyses of emission differentiation mechanisms and regional response variations under diverse human activities remain lacking.

This study extends existing frameworks by incorporating multidimensional human activity impacts on emission patterns. We investigate dynamic provincial carbon emission characteristics through integrated dynamic time series analysis and hierarchical clustering. By examining contributions from food, water, housing, transportation, and energy sectors to total emissions, we explore

spatial differentiation mechanisms across emission types. This study selects five key sectors of food, water, housing, transportation and energy as the analytical dimensions of carbon emissions, because they cover the core areas of basic human life and production activities, and each has obvious carbon emission characteristics and driving mechanisms. In recent years, the proportion of these sectors in total carbon emissions and their changing trends have become the focus of regional low-carbon transformation policies (Zhang et al., 2023; Li et al., 2024; Wang and Chen, 2025). This approach provides precise scientific evidence for formulating differentiated mitigation policies. Industrial carbon emissions warrant particular attention given their profound ecological and public health implications. Through temporal evolution pattern analysis, we reveal provincial emission trajectories and regional disparities. Specifically, t dynamic time warping (DTW) captures temporal dependencies and fluctuation characteristics across emission categories (Wen et al., 2024), enabling comprehensive trajectory measurement to inform policy formulation. Hierarchical clustering techniques (Sabbir, 1998) group provinces with similar emission patterns, facilitating identification of distinct emission clusters through regional comparisons. This research enriches China's carbon emission theoretical framework while providing policymakers with actionable references for climate mitigation strategies. Furthermore, it establishes methodological foundations for future exploration of carbon emission-socioeconomic relationships.

2 Method

2.1 Data source

This study is conducted with comprehensive and reliable data on carbon emissions at the provincial level, obtained from reputable sources such as the National Bureau of Statistics of China and relevant governmental departments. Our data is collected by Python and Java web parsing tools with pre-process of filtering and cleaning. The industrial energy and carbon emission data comes from China Carbon Emission Accounts and Datasets for Emerging Economies (CEADs, 2023) and the IPCC (Intergovernmental Panel on Climate Change) National Greenhouse Gas Inventory Guidelines (2001-2020) (IPCC, 2021) (Tibet, Taiwan, Hong Kong, and Macao are not available). Data on energy classification and consumption of each province are obtained from China Energy Statistical Yearbook 2001–2020 (Companies and Markets, 2008). Population and GDP data comes from China Statistical Yearbook (Research and Markets, 2008). Considering the data availability and completeness, our study focuses on the data during the target years between 2001 to 2019 including 30 provinces and municipalities from mainland China. Due to large portion of missing data, Tibet, Hong Kong, and Macao are excluded from investigation areas.

2.2 Calculation of spatial characteristics of interprovincial carbon dioxide emissions

The spatial characteristics of interprovincial carbon dioxide ($\rm CO_2$) emissions are typically calculated through spatial autocorrelation analysis (identifying spatial aggregation patterns of emissions), hotspot analysis (locating high/low value clusters), and spatial regression models (SLM (Spatial Lag Model), SEM (Spatial Error Model), geographically weighted regression) to explore spatial effects.

These methods are combined with spatial weight matrices (adjacency, distance, or economic linkages) to quantify interprovincial associations, supported by GIS tools for visualization and modeling. Compared to GWR (spatial-only) and TWR (temporal-only), GTWR integrates spatio-temporal non-stationarity by weighting observations based on spatial proximity and temporal proximity (Yao et al., 2021; Wu et al., 2021). This is critical for China's provincial emissions, where Moran's I shifted from positive (2010–2014) to negative (2015–2019), indicating weakening spatial dependence and strengthening temporal heterogeneity (Table 1). GTWR's dual kernel function captures such dynamics, enabling unbiased estimation of drivers like energy intensity in Inner Mongolia (spatial hotspot) post-2015.

2.3 Carbon emission intensity analysis and prediction

The algorithm of the model mainly involves the analysis of the least squares method of statistics. A linear regression analysis was performed on year-carbon emissions and year-food and water-related emissions. A comparative analysis of the two. And then to predict the country 's carbon emissions. And for the convenience of the next calculation, the carbon emissions of the four categories of food, water, housing and transportation in the country are also predicted. At the same time, in order to analyze the impact of food, water, housing, and transportation on the total carbon emissions, a multiple regression analysis was also performed with the total emissions. The above analysis and modeling are carried out for the data of the whole country and 30 queried provinces.

The data processing in the above regression analysis mainly uses python language and java language. For data in standard message format, it mainly uses alibaba's fastjson toolkit to split and reorganize messages, extract and calculate data, and finally output. For the most primitive data, scrapy crawler technology is needed to obtain keyword pages. For the analysis of linear regression by putting the processed data into the model, the third-party scientific computing software package pandas and statsmodels. Api of python are mainly used to train and calculate the data, so as to obtain the result formula. For the high-precision calculation in the data, python 's accuracy package is used to ensure the calculation accuracy. It is also necessary to use the third-party software tools ArcGis and python's graphics toolkit for visual analysis and display of model results.

2.4 Data preparation

Carbon Emission and GDP data are characterized into the first, second, and tertiary industry with 44 sub-level industries, according

TABLE 1 Results of multicollinearity analysis.

| Coordinate | Tolerance | VIF |
|------------|-----------|-------|
| x1 | 0.237 | 4.216 |
| x2 | 0.226 | 4.426 |
| x3 | 0.658 | 1.521 |
| x4 | 0.488 | 2.049 |

VIF values <5 for all drivers (Food: 4.216; Water: 4.426; etc.) confirm no severe multicollinearity (Hair et al., 2010).

to the provisions on the division of three industries posted by the National Bureau of Statistics in 2012 (Xu, 2019). Unclassified carbon emission sources such as the carbon emissions in daily life from urban, rural area and other sources are also removed from the analysis process.

Population growth is broadly used as one of the essential factors to evaluate regional carbon emission, and population weighted factors are commonly used in economitric-based models, such as GDP per capita and carbon emission per capita. However, our study starts from the absolute sizes of industrial carbon emission and GDP over observation time horizon. In order to eliminate the effect of population growth, a new factor, Average Carbon Cost of Production (ACCP), is proposed for a better understanding of the evolution of carbon emission paths with provincial level industrial data. ACCP is defined as yearly regional GDP divided by corresponding amount of carbon emission (Unit: Tons of Carbon Dioxide Emitted per 10,000 CNY). It is a simple but strong indicator for the relationship between production and carbon emission, as ACCP allows direct comparison on the longitudinal observations from different observation time by mathematically.

2.5 Clustering methodology

Clustering is an unsupervised learning technique used to explore and identify the common patterns for study population. There have been plenty of studies on cross-sectional carbon emission data with clustering. Li et al. (2022) used a combination of static and dynamic indices as the inputs for clustering. Static includes population, Economic level, industrial structure, and dynamic indices includes the growth in population, GDP, city expansion, and carbon emission. He et al. (2022)'s study used selected factors of GDP per capita (GPC), GDP intensity of power (GIP), TPG energy efficiency (TEE), and share of non-fossil power (SNP) from Logistic Mean Divided Index (LMDI) with a K-means clustering. Similarly, Jiang et al. (2017) combines a multi-layer LMDI model with hierarchical clustering. One major deficiency of the cross-sectional analysis is that data is observed from each single time point, which cannot reflect the time lagging and speed of carbon emission paths. For example, local carbon neutral policy might be promoted to other regions and leading to similar carbon emission paths but with temporal differences. To capture the overall path similarity, Dynamic Time Warping (DTW) is introduced as the similarity measure for comparing two times series. Considering the fact that it is hard to define an interpretable "central series" for multivariate time series data under DTW distance, centroidbased clustering algorithms, such as widely used K-Means, are no long applicable here.

Dynamic Time Warping (DTW) is employed as an algorithmic approach aimed at quantifying the similarity between two temporal sequences that exhibit variability in terms of pace (Salvador and Chan, 2007). Applications of DTW have been found in the analysis of video sequences, audio streams, and graphic data, which underlines its versatility in handling diverse forms of data while maintaining high levels of accuracy in identifying temporal correlations. The DTW is formulated as following: Given two times series X and Y of length n and m, where (Equations 1, 2),

$$X = x_1, x_2, ..., x_n, Y = y_1, y_2, ..., y_m$$
 (1)

a warp path W is a list of index pairs with length K given by.

$$W = [w_1, w_2, ..., w_K] \text{ with } w_k = (i_k, j_k), i_k \in \{1, ..., n\}, j_k \in \{1, ..., m\}$$
(2)
$$s.t. w_k - w_{k-1} \in \{(1,0), (0,1), (1,1)\} \text{ for } \forall_k \in [1:K]$$

The optimal warp path is the warp path W has the minimum-distance, where the distance of a warp path is (Equation 3)

Dist(W) =
$$\sum_{k=1}^{k=K} d(x_{w_{ki}}, y_{w_{kj}})$$
 (3)

And d is a distance function d: $Rdim(x) \times Rdim(y) \rightarrow R1$. For this study, we use Euclidean distance as the distance function for calculation. Then distance of the optimal DTW path is used as the dissimilarity measure between X and Y. Instead of vanilla DTW, we use an accurate approximation to DTW with higher computation efficiency provided by Salvador and Chan (2007). Notice that all the above calculation is based on one-dimensional time series, but it can be easily expanded to multivariate time series by calculating the Euclidean distance for each xt and yt $\in Rz$, where $z \in Z > 1$.

Agglomerative Hierarchical Clustering (AHC) is a bottom-up algorithm aiming to partition data points into distinct clusters based on their similarities or dissimilarities. The AHC algorithm first assumes individual observations as different clusters with only one member, then iteratively merges two clusters until there is only one cluster left. Linkage functions as measurements of similarities between clusters determines the clusters to be merged. We used the unweighted average linkage function as following (Qin et al., 2019):

$$L(A,B) = \frac{1}{NA^*NB} \sum_{X \in A} \sum_{Y \in B} dDTW(X,Y)$$
 (4)

Where A, B are two different cluster sets, N is the cardinality of given set. This linkage function minimizes the average distance of each observation of the two sets (Equation 4). From above definition, it is easy to see that AHC only depends on pairwise distance calculation between observations and avoids the problem of missing centroids. Moreover, AHC forms a tree structure usually interpreted with dendrograms reflecting the cluster merging process, which enables a systemic analysis for different regions.

2.6 Data processing

DTW-AHC is implemented on two datasets, with each of the dataset as a three-dimensional multivariate time series. First dataset is from a combination of Total Carbon Emission (TCE, in tons), Gross Domestic Production (GDP, in 10,000 CNY), and Average Carbon Cost of Production (ACCP). Another dataset is the proportions of carbon emission from the production of primary, secondary, and tertiary industries to the total amount of carbon emission for each province region between 2001 and 2019, giving 30 three-dimensional time series of length 19 years. Noticing that Euclidean distance are used in the DTW for the distance measure

between observations, it is necessary to apply a transformation on each dimension, respectively, to the same scale in order to carry the same "dissimilarity" level (Jiang et al., 2017). A cross-sectional standardization is used to equally scale each dimension, defined as following (Equation 5):

$$Z_{ti} = \frac{X_{ti} - X_t^-}{\sigma X_t} \tag{5}$$

and in this case:

$$Z^{\rightarrow} = \left\langle z_{1ti}, z_{2ti}, z_{3ti} \right\rangle = \left\langle \frac{x_{1ti} - \sum_{i=1}^{n} x_{1ii}}{\sigma X_{1ti}}, \frac{x_{2ti} - \sum_{i=1}^{n} x_{2ii}}{\sigma X_{2ti}}, \frac{x_{3ti} - \sum_{i=1}^{n} x_{3ii}}{\sigma X_{3ti}} \right\rangle (6)$$

Where z_{1ti} is the transformed variable of first dimension for province i in year t, x_{1ti} is the first raw variable for province i in year t, σ_{x1t} is the standard deviation of first raw variable for all provinces in year t, and n=30 for 30 provinces in the study population (Equation 6). Then DTW is applied for each dataset to calculate the pairwise distance between series. Obtained the distance matrix D of size (30, 30), it is scaled by its maximum to interval [0.1]. These two distance matrices along with Average Linkage function are feed into the AHC algorithm for training to obtain clusters.

3 Result

3.1 Covariance analysis of CO₂ emissions

3.1.1 Spatial autocorrelation analysis

In order to better assess the driving mechanisms of $\rm CO_2$ concentration changes as a whole, a spatio-temporal weighted regression model (SGTWR) was measured in this paper for five types of drivers, including food, water, domestic, transportation, and energy. Taking carbon emissions as an example, it can be seen from Figure 1 that carbon emissions in each domain show unevenly distributed spatial and temporal differences, and carbon emissions have spatial and temporal non-smoothness. Based on the data of carbon dioxide emissions in total, food, water, domestic, transportation, and energy in China from 1996 to 2019, a spatio-temporal weighted regression model (SGTWR) was used to estimate the influencing factors of carbon emissions in different regions in different periods. The results of multicollinearity show that the reporting model is stable and reliable (Table 1).

For higher data reference value, we calculated the Moran's I index values of total carbon emissions for each province in China from 2010 to 2019 using ArcGIS software, and the results are shown in Table 2. The data indicate the existence of spatial correlations and spatial aggregation patterns, indicating that the spatial aggregation of carbon emissions in each province and city has been decreasing and the trend of discrete distribution is obvious. The weakening of spatial agglomeration of carbon emissions after 2015 may be related to the regional differentiated emission reduction policies, industrial structure adjustment and renewable energy promotion proposed in the national "13th Five-Year Plan". In particular, the eastern coastal

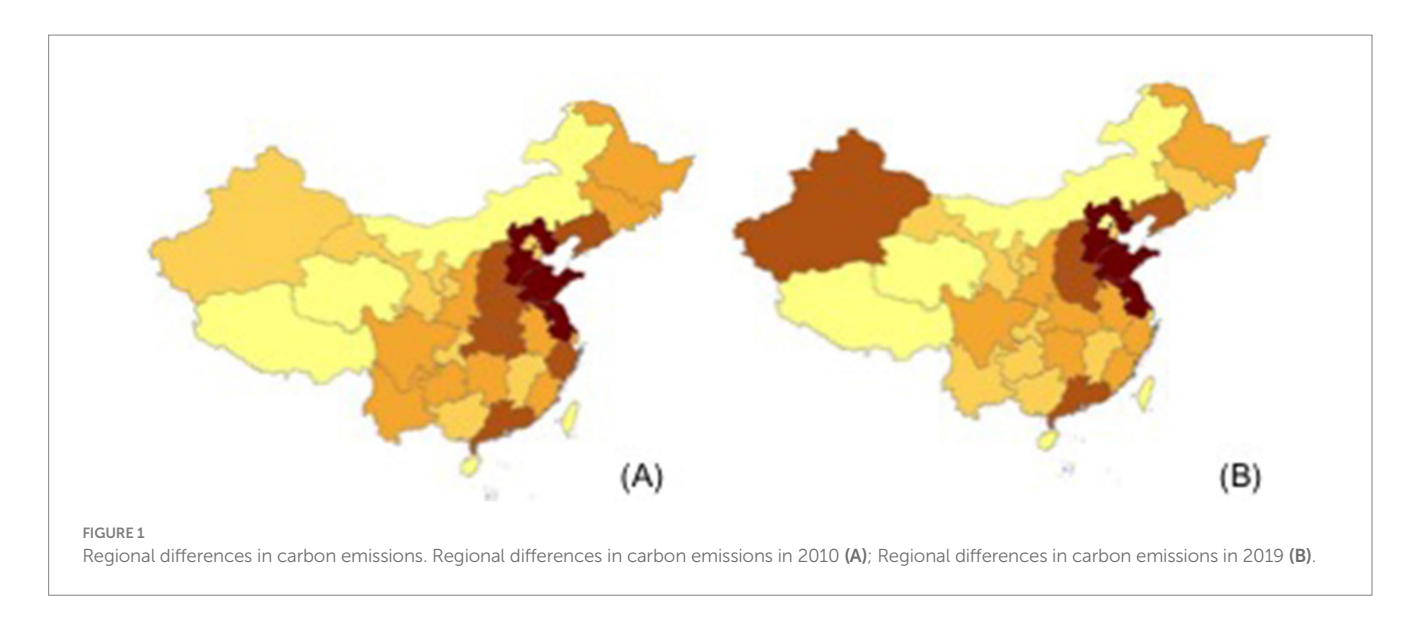


TABLE 2 Moran's I index of provincial CO_2 emissions from 2010 to 2019 in China.

| Coordinate | Moran's I index | z score | p value |
|------------|--------------------|-----------|----------|
| 2010 | 0.074565 | 1.310702 | 0.189958 |
| 2011 | 0.05805 | 1.112797 | 0.265796 |
| 2012 | 0.043836 | 0.949007 | 0.342617 |
| 2013 | 0.024718 | 0.718167 | 0.472655 |
| 2014 | 0.020622 | 0.667049 | 0.504741 |
| 2015 | -0.048076 | -0.15973 | 0.873094 |
| 2016 | 0.009056 | 0.533264 | 0.593851 |
| 2017 | -0.069858 | -0.438938 | 0.660707 |
| 2018 | -0.005855 | 0.356827 | 0.721221 |
| 2019 | -0.010388 | 0.302397 | 0.762349 |

areas have achieved a slowdown in emission growth through industrial upgrading and energy structure optimization, while the central and western regions still rely on traditional energy, resulting in enhanced spatial heterogeneity.

3.1.2 Analysis of carbon emission dynamics in multiple sectors

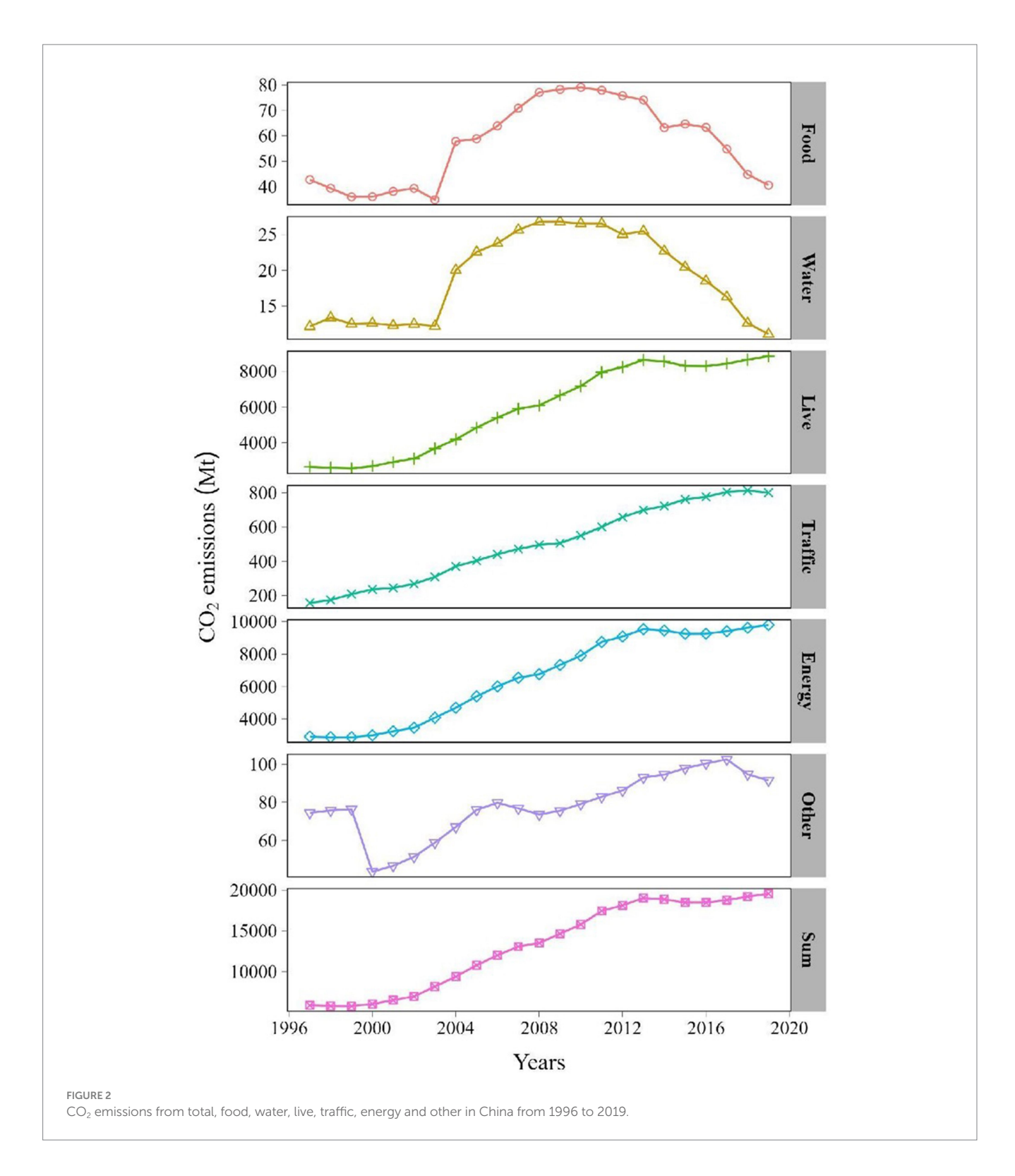
The statistical results showed that the individual coefficients of food, water, living, transportation, and energy drivers have large variance. It indicates that when studying regional carbon emission scale and carbon emission intensity, each carbon emission driver has a large variation, and it is necessary to discuss the spatial and temporal heterogeneity in carbon emission scale and carbon emission intensity from each field of in-depth analysis, and SGTWR has obvious advantages by considering both temporal and spatial differences.

As can be seen from Figure 2, the total carbon emissions in China from 1996 to 2019 show a continuous increase. It increased from 2935.92 Mt. in 1996 to 10864.41 Mt. in 2019, with an average annual growth rate of 5.85%. The overall phase can be divided into 4 stages according to the characteristics of carbon emission dynamic change. The first stage is 1996–2000, which is characterized by small carbon

emissions and slow growth rate, with carbon emissions increasing from 2935.92 Mt. in 1996 to 3053.31 Mt. in 2000, with an average annual growth rate of 0.98%. The second stage is from 2000 to 2007, the growth rate of carbon emission is obviously accelerated, from 3053.31 Mt. in 2000 to 6822.27 Mt. in 2007, with an average annual growth rate of 12.17%. The third stage is 2007–2013, when the growth of carbon emissions slowed down: from 6822.26 Mt. in 2007 to 9778.95 Mt. in 2013, with an average annual growth rate of 6.18%, with China's overall carbon emissions reaching the highest in 2013. Phase 4 is from 2013 to 2019, where carbon emissions show a slight decreasing trend: from 9778.95 Mt. in 2013 to 10864.41 t in 2019, with an average annual reduction rate of 1.77%. Analyzing several categories of drivers in terms of food, water and living, we can see that carbon emissions from energy consumption are in line with the trend of overall carbon emissions. This indicated the dominant role of carbon emissions from energy activities. Carbon emissions from daily life and transportation also show a gradual increase from 1996 to 2019, and their growth trend is not very different from the overall carbon emissions. Such a change is probably due to the increase in population and the significant improvement in living conditions. Interestingly, around 2012, CO₂ emissions from food and water start to decline, to 10 Mt. and 10 Mt., respectively, by 2019. This may be due to the change in population size and the development of environmental awareness. The decline in food and water sector emissions is mainly due to the promotion and application of green technologies such as water-saving irrigation technology, precision fertilization, sewage treatment and reuse. Especially in major agricultural provinces such as Henan and Shandong, these technologies combined with policy subsidies have significantly reduced carbon emissions per unit of output.

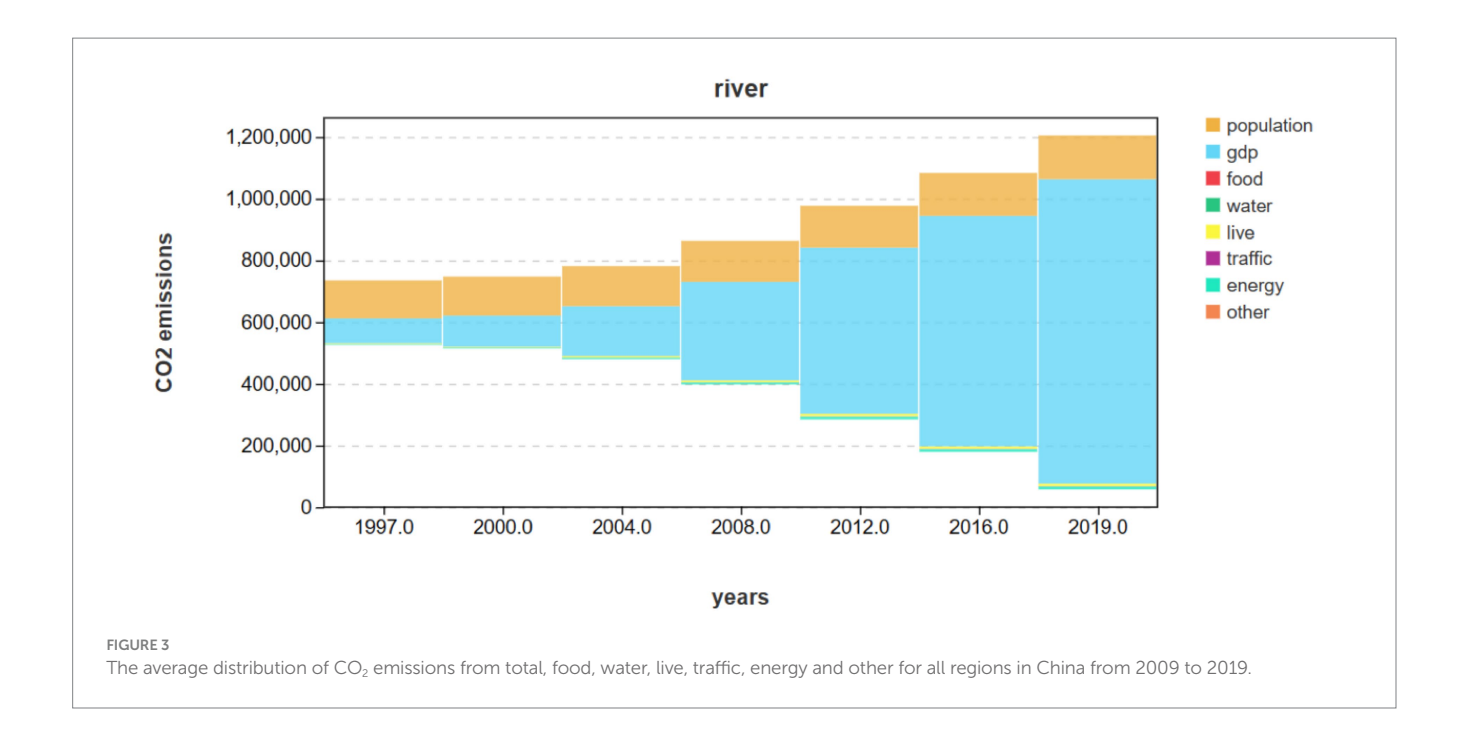
3.1.3 Analysis of shift of carbon emission focus

In order to further analyze the relationship between each driver and the spatial distribution of CO_2 concentration, the carbon dioxide emission rates from 1996 to 2019 were plotted for different types of CO_2 emissions in China, such as total, food, water, domestic, transportation, and energy. In terms of total carbon emissions from 1996–2019 (Figure 3), it is clear that GDP has the most significant impact on the total. We can see that population is also a factor with a



large degree of influence. Compared to population and GDP, the five drivers we focus on, such as water, food, and transportation, have a smaller impact on the total amount of carbon emissions during 1996–2019. In contrast, the carbon emissions from live and water have a relatively large proportion in terms of emissions. This trend is mainly due to the population growth and economic development of the society, which brought about a significant increase in the standard of living, resulting in more the carbon emissions from live. At the same

time, we cannot deny that the carbon emissions from water are mainly due to the ecological changes of rivers in mainland China (Raymond et al., 2013). Water is the more significant biogeographic link between continents, oceans and atmosphere, therefore, when analyzing water as a driver, we need to integrate the net ecosystem production of Chinese rivers and the impact of CO_2 emissions on organic carbon and carbon emissions (Song and Wang, 2021). For both food, traffic, the changes in the relative total amount of carbon emissions are not



significant. Combining the analysis results in Figure 3, we believe that Different types of carbon emission from total, food, water, live, traffic, energy and other in China from 2009 to 2019 all have an increasing trend, but the magnitude of the increase and the change This is mainly due to the inconsistent trends in energy consumption, industrial structure, population and GDP.

3.2 Carbon emission intensity analysis and prediction

3.2.1 Analysis of spatial heterogeneity of carbon emission intensity

The contributions of live, water, traffic, energy, and food to carbon emission intensity are different, and the spatial spillover effects of different drivers vary greatly. Taking carbon emission intensity as an example, it can be seen from Figure 3 that carbon emission intensity shows an uneven distribution of spatial and temporal differences, and carbon emission has spatial and temporal non-stationarity (Figure 4).

Based on the provincial regional panel data from 1996 to 2019, the GTWR is applied to estimate the parameters of carbon emission drivers for each region from time to time, and the results of the spatiotemporal geographically weighted regression model with the natural log ln(CS) of carbon emission intensity as the explanatory variable for the parameters of carbon emission scale drivers are described in Table 3. The optimal bandwidth of the GTWR model is 2.88, which is based on the Gaussian function of the spatio-temporal weighting function. The large variation in the coefficients of live, water, traffic, energy, and food indicates that there are large differences in the drivers of carbon emissions in each province when studying regional carbon emissions intensity, and the spatial and temporal heterogeneity in regional carbon emissions intensity needs to be considered locally. Resource dependent clusters (such as Shanxi and Inner Mongolia) face challenges such as high coal dependence, single industrial structure, and high ecological restoration pressure, and need to focus on promoting the application of CCUS technology and ecological compensation mechanisms. Rapid growth clusters need to prevent difficulties in decoupling economic growth from emissions, and it is recommended to strengthen the construction of green infrastructure.

Through the global Moran 's I test, China 's inter-provincial CO_2 emissions from 2009 to 2019 showed a significant positive spatial autocorrelation (I > 0, P 2.58), while the western region was the cold spot area. From 2009 to 2019, the spatial distribution of per capita CO_2 emissions shows a significant increase in emission intensity in the eastern coastal provinces (Figures 5A–C), especially in energy-intensive industrial concentration areas, due to the adjustment of industrial structure in the central and western regions, the growth rate of emissions in some provinces has slowed down. From the perspective of sectors, the spatial expansion of transportation and residential carbon emissions is the most significant (Figures 5D–F), which is closely related to the urbanization process and the growth of private car ownership.

3.2.2 Regression curves and forecast for CO_2 emissions

The regression curves for CO₂ emissions in China reveal strong positive correlations between total emissions and GDP and population growth, indicating economic expansion and urbanization as dominant drivers. Energy-related emissions exhibited the highest elasticity to GDP, driven by coal-dependent industrialization, particularly post-2008. Further analysis shows that coal-fired power remains the main source of emissions from the energy sector, especially in the northern provinces. Road freight and private vehicle growth are the main drivers of traffic emissions. It is suggested that future research should subdivide energy types and transportation modes to more accurately identify emission reduction priorities. Traffic emissions showed the steepest growth trajectory, aligning with rising private vehicle ownership and freight demand. Water and food-related emissions remained stable or declined post-2016, reflecting technological improvements, while energy and traffic sectors dominated structural

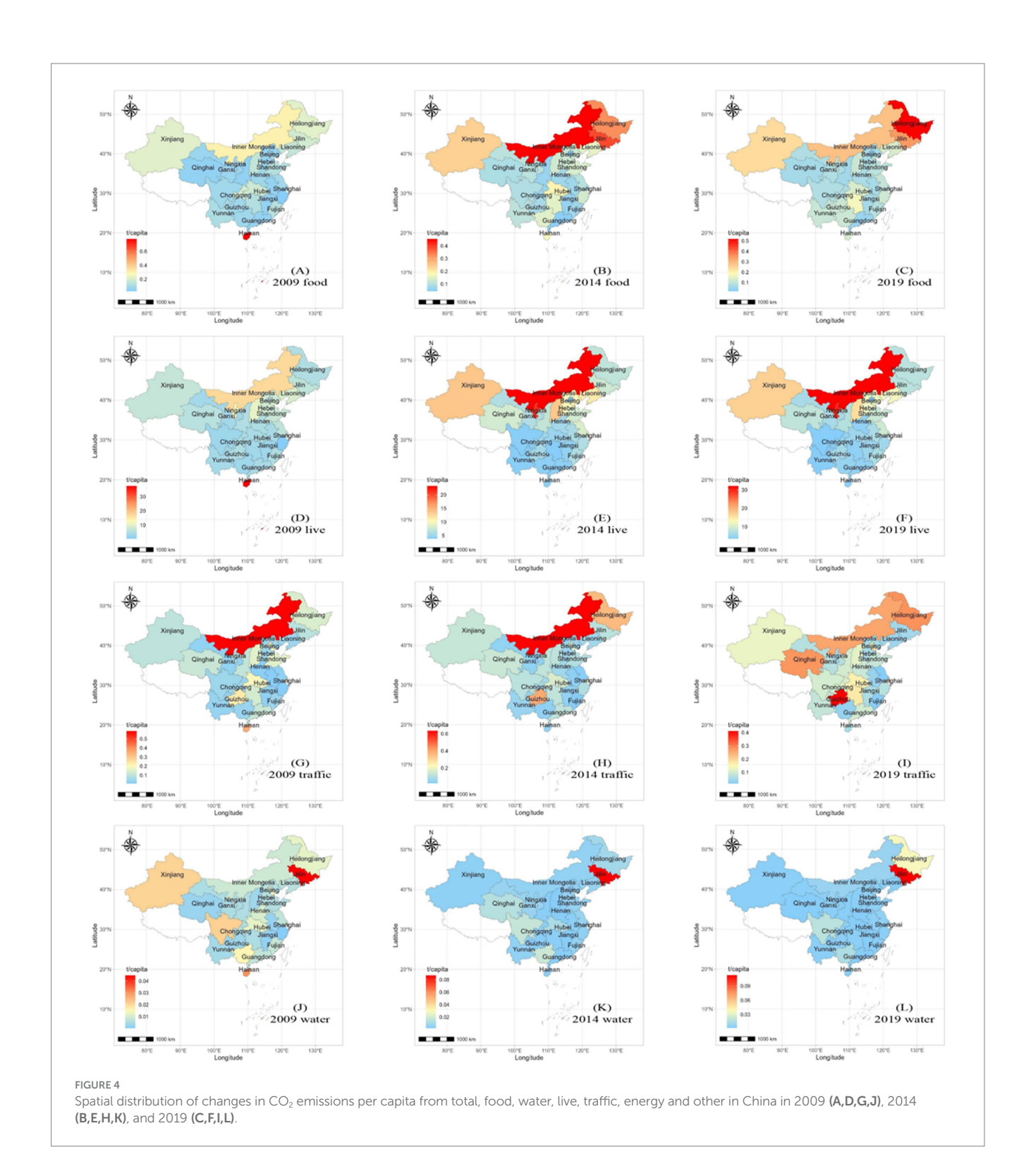
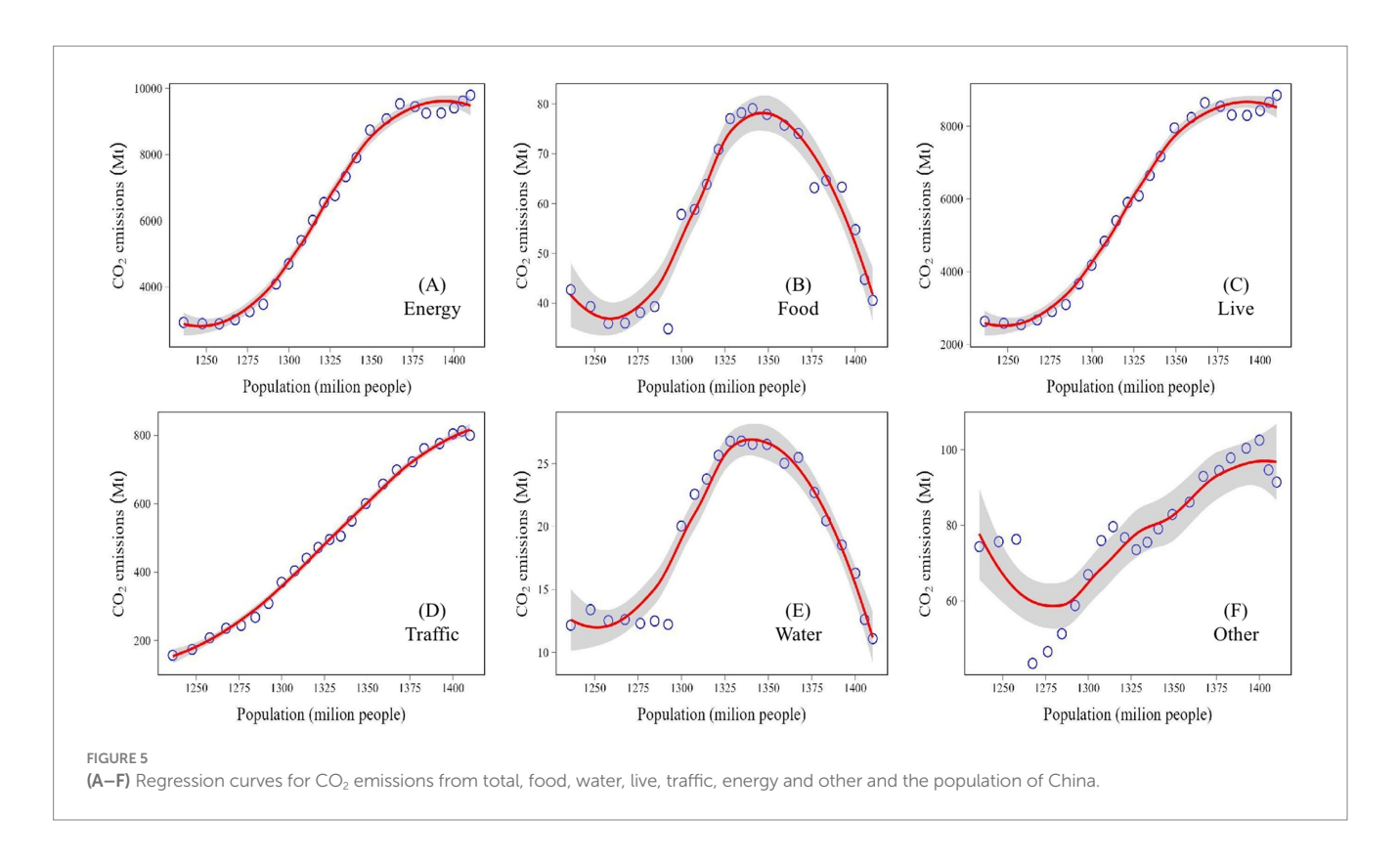
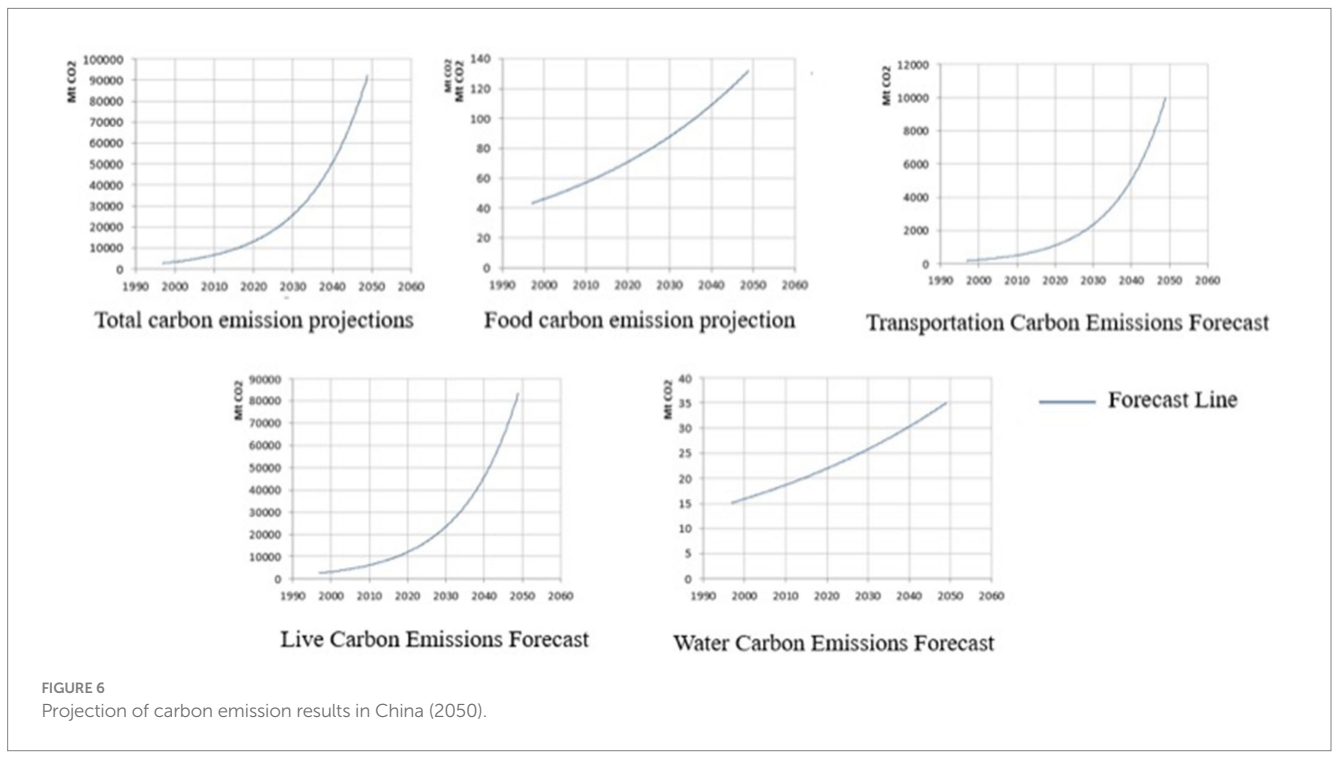


TABLE 3 The natural log ln(CS) of the carbon emission scale as the explanatory variable of GTWR parameter estimation descriptive statistics.

| Coordinate | Min | ½ quartile | Median | ³∕₄ quartile | Max | Quartile distance |
|------------|----------|------------|----------|--------------|----------|----------------------|
| X1 | -0.55065 | 0.008734 | 0.020941 | 0.03758 | 0.371038 | 0.028847 |
| X2 | -0.00706 | 0.005129 | 0.006545 | 0.009372 | 0.050323 | 0.004243 |
| Х3 | -2039.69 | -80.921 | -93.936 | -53.2358 | 877.549 | 627.6856 |
| X4 | -273.349 | 253.275 | 421.5895 | 1177.19 | 1953.71 | 923.915 |
| constant | -571.953 | -135.49 | -5.2088 | 1.641543 | 1456.15 | 137.131 |



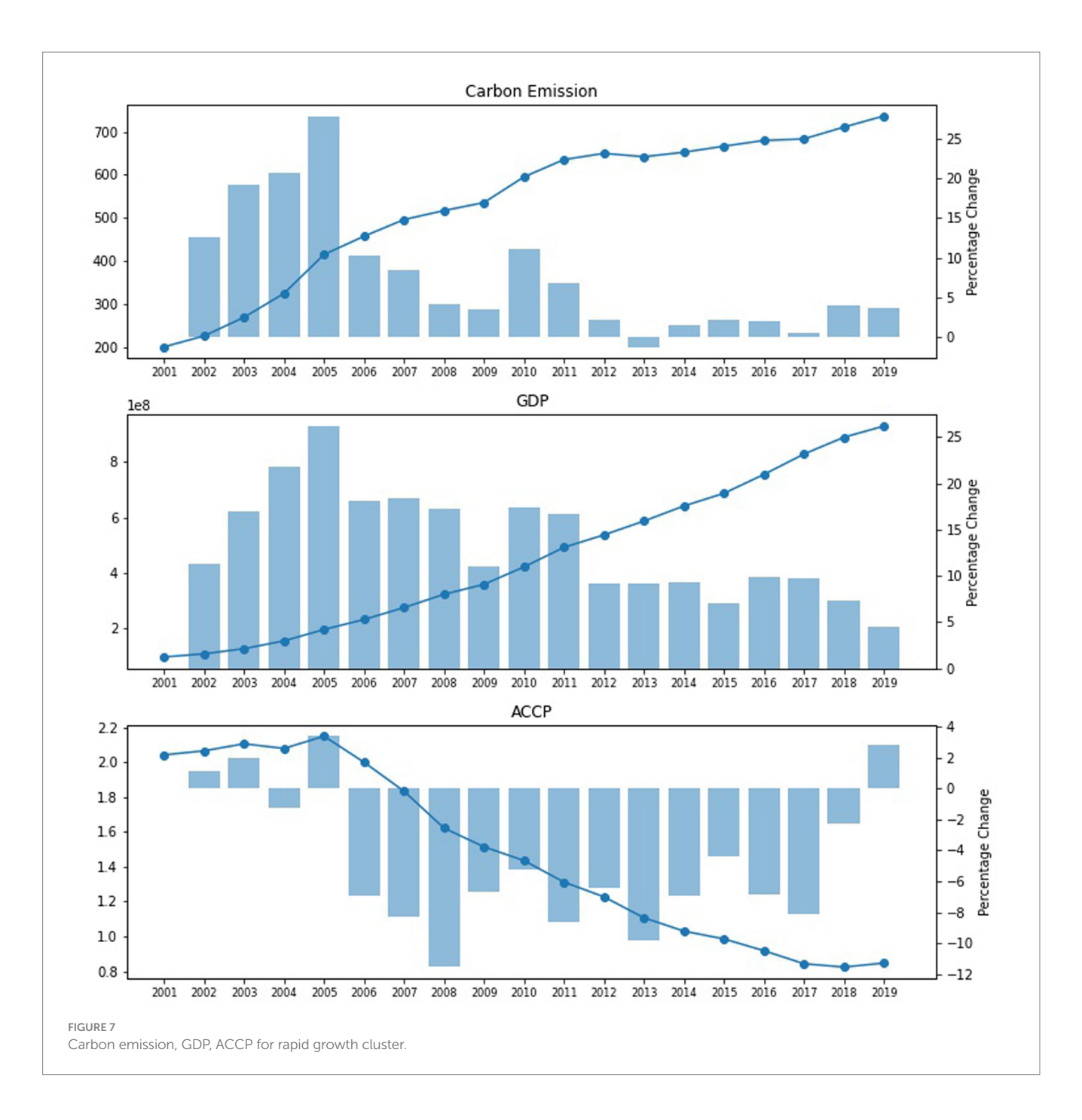


inertia. These results underscore the need for region-specific decarbonization policies, prioritizing energy transition (renewables), transportation electrification, and green urban planning to decouple emissions from economic growth (Figure 6).

We make a forecast of each carbon emission data in 2050 according to the analysis results of the data and the future development trend in accordance with the calculation law, and the specific forecast

trend is shown in Figure 7. Using multiple linear regression analysis, the national carbon emissions are all on the rise, with housing and transportation accounting for a significant proportion, and energy conservation and emission reduction becoming a national effort (Figure 6).

Cities played a vital role in achieving China's carbon peak and carbon neutrality goals. However, due to various factors, there are



significant differences in carbon emissions in different cities. Therefore, carbon peak actions at the city level need to be distinguished according to different types of cities. In this study, the classification method is used to classify Chinese cities, which provides a classification model for the carbon emission path nationwide.

3.3 TCE-GDP-ACCP clustering

Based on the results of hierarchical clustering on TCE-GDP-ACCP, four clusters can be visualized with a dendrogram showing the hierarchical structure for each cluster. From the analysis of their carbon emission, GDP, and ACCP paths, we classify the four clusters

as "Rapid Growth Cluster," "Low-Carbon Exemplar Region Cluster," "Typical Growth Cluster," and "Resource Dependent Cluster" respectively with their children regions shown in Table 4.

In order to illustrate the dynamic path evaluation of each cluster, we divide the data to two sub-periods with the first period from 2000 to 2011 and the second period from 2012 to 2019. This is from empirical observation that 2011 is the turning elbow for the carbon footprint paths of all four clusters. The average percentage changes of Total Carbon Emissions, industrial GDP, and ACCP for two periods are reported in Table 5 for comparison.

3.3.1 Rapid growth cluster

"Rapid Growth Cluster" includes provinces characterized by high economic growth and large industrial carbon emission amount in

China, including Jiangsu, Guangdong, and Shandong, which plays an important role in the economic development and the process of industrialization in China. From Figure 8, GDP of this cluster showed a powerful trend of growth and remains the highest among the four clusters. Based on the data averaging from 2001 to 2019, Rapid Growth Cluster contributed 55.58% of the total GDP. In the first period from 2001 to 2011, the rapid growth cluster's GDP grows from 980 billion to 4,920 billion in 11 years, with second highest average annual growth rate of 17.51%. In the period of 2012 to 2019, the GDP growth trend of this cluster slows down but also remains the second highest average annual growth rate of 8.56%. This reflects the strong economic strength and sustained development momentum of regions in this cluster.

At the same time, this rapid economic growth is accompanied by a corresponding increase in energy consumption and carbon emissions, leading to a high level of total carbon emissions. The total industrial carbon emission amount of "Rapid Growth Cluster" also maintains at the highest with an average proportion of 43.34% over the 19 years. In 2001, the total carbon emission amount of the rapid growth cluster is 200.61 million tons and increases to 736.23 million tons in 2019, with annualized average growth rate of 12.45 and 1.88% for the first and second sub-periods.

The contradiction between economic growth and carbon emission reduction brings up the challenging problem for many developing countries during their rapid development phase, where economic growth is achieved by the cost of rising energy consumption and environmental pressures. The process of industrialization and urbanization caused the significantly rising demand for energy with consequential increase in carbon emissions. At the same time, traditional energy sources are difficult to be fully replaced by cleaner energy sources in the short term,

TABLE 4 TCE-GDP-ACCP cluster classification.

| Cluster name | Children |
|-----------------------------|--|
| Rapid growth cluster | Jiangsu, Guangdong, Shandong |
| Low-carbon exemplar cluster | Beijing, Shanghai, Fujian, Sichuan, Hunan, Hubei |
| Typical growth cluster | Anhui, Heilongjiang, Guangxi, Jiangxi, Chongqing, Tianjin, Shaanxi, Jilin, Yunnan, Liaoning, Henan, Zhejiang, Hebei, Xinjiang, Guizhou, Qinghai, Gansu, Hainan |
| Resource dependent cluster | Shanxi, Inner Mongolia, Ningxia |

TABLE 5 Cluster statistics.

| Variable | es | Cluster 1 | Cluster 2 | Cluster 3 | Cluster 4 |
|----------|-----------|--------------|--------------|--------------|--------------|
| Average | Δ ΤСΕ | 0.1245 | 0.1024 | 0.1129 | 0.1356 |
| Over | Δ GDP | 0.1751 | 0.1632 | 0.1706 | 0.2273 |
| 2001- | Δ ACCP | -0.0420 | -0.0527 | -0.0479 | -0.0758 |
| Average | Δ ΤСΕ | 0.0188 | -0.0007 | 0.0173 | 0.0354 |
| Over | Δ GDP | 0.0826 | 0.1031 | 0.0769 | 0.0407 |
| 2012- | Δ ACCP | -0.0525 | -0.0946 | -0.0460 | -0.0092 |

thus inevitably bringing a huge challenge in the process of carbon neutral. With urbanization and increasing productivity demand in developing countries, it is essential to answer the important question behind the "Rapid Growth Cluster": how to achieve economic growth while realizing the control and reduction of carbon emissions (Figure 7).

3.3.2 Low-carbon exemplar cluster

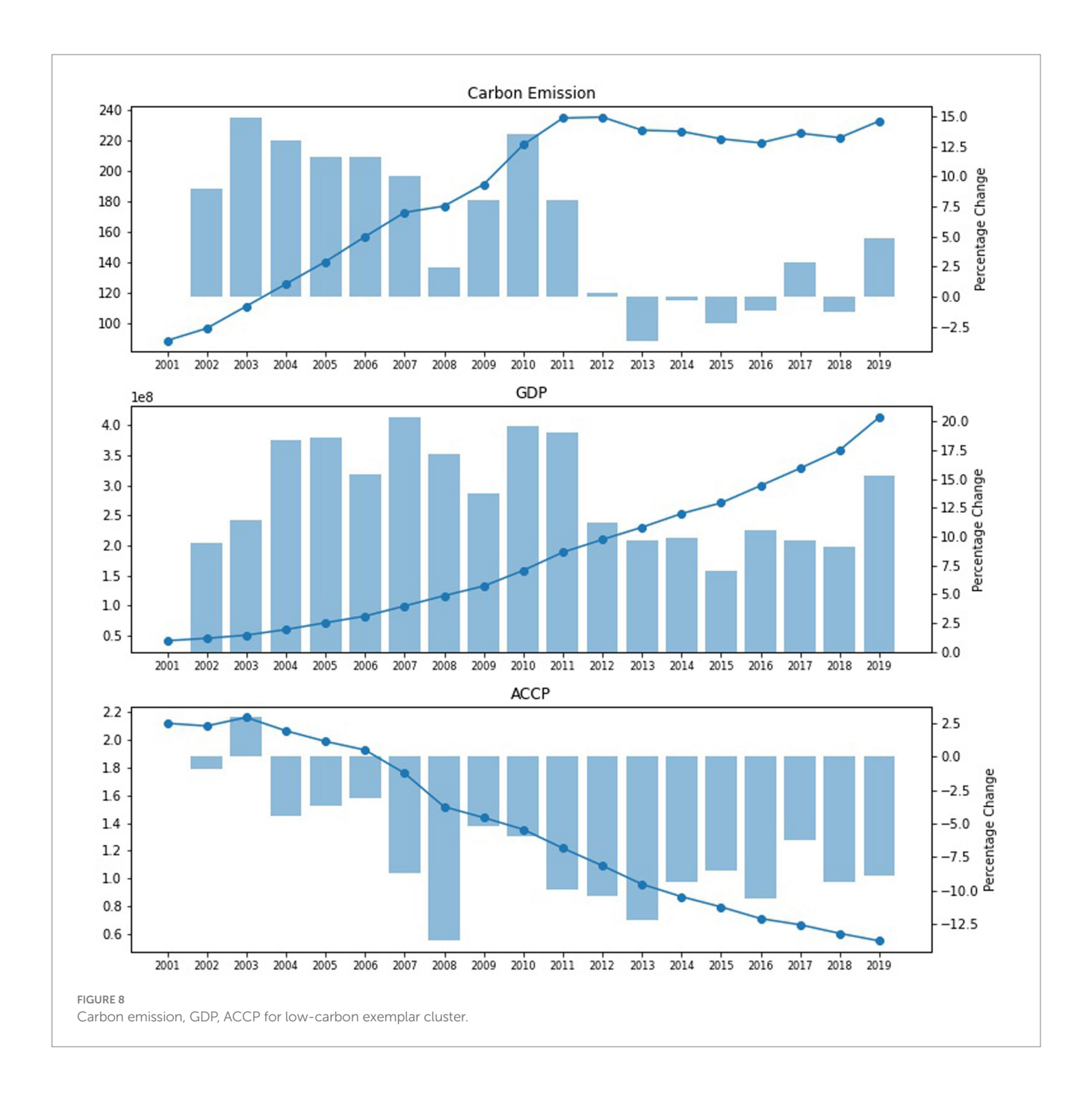
The Low-Carbon Exemplar cluster represents the regions with significant progresses in carbon-natural process as well as maintaining rapid GDP growth. The GDP of this cluster shows a steady growth power, increases from 410 billion in 2001 to 4,135 billion in 2019, with average growth rates of 16.32 and 10.31% for the two sub-periods, respectively. During the sub-period from 2012 to 2019, while the average growth rate of GDP slows down for Chinese economy, this cluster achieves the highest average annual growth rate among four clusters, evidencing the great successes with respect to economic development in these regions. As for carbon emission, it is remarkable that, starting from 2011, the industrial carbon emissions amount started to decline and maintains at the level of approximately 220 million tons per year, indicating an important step toward greener and more sustainable economic practices. The average annual growth rate of industrial carbon emission changes from 10.23% in the first sub-period to -0.06% in the second sub-period, which is also the only cluster with declined carbon emission trend.

Furthermore, an interesting aspect exhibited by this cluster is the significant reduction in the Average Carbon Cost of Production (ACCP) since 2004. The ACCP ratio drops from 2.11 in 2001 to 0.55 in 2019, with an average annual decreasing rate of 7.2%. This reduction in ACCP demonstrates the successful alignment of economic activities with environmental goals, further proving the effectiveness of carbon reduction strategies within Low-Carbon Exemplar Cluster. The confluence of these trends, reduced carbon emissions, lower ACCP values, and sustained GDP growth, underscores the effectiveness of the carbon reduction policies implemented by these regions. It not only contributes to the country's carbon reduction targets, but also sets a precedent for other regions in their efforts to find a balance between the pursuit of economic prosperity and environmental responsibility (Figure 8).

3.3.3 Resource dependent cluster

Resource Dependent Cluster is an important group in cluster analysis, which has distinctive characteristics in carbon emission and economic growth. Inner Mongolia, Shanxi, and Ningxia, as regions that rely on resource-based industries, show similar trends in the following aspects. The most noticeable difference between this cluster and the others is the extremely high ACCP ratio. The ACCP of this cluster remains the highest across the period from 2001 to 2019. In 2001, its ACCP is approximately 11.22 (estimated with the imputed missing data of Ningxia), which is 3 to 5 times higher than other clusters, and the ratio is 4.45 in 2019, increasing to 7 times higher than Low-Carbon Exemplar Cluster. This cluster also takes a huge proportion of the net carbon emission amount in China, grows from 22.69% in 2001 to 28.99% in 2019, while its corresponding GDP only takes 6.73 and 7.44% of the total GDP. Combining these features of Resource Dependent Cluster, it determines the fact how to manage the carbon emission in these regions would be a huge challenge for achieving the carbon neutral goal of China.

To address the issues of this cluster, we look into the industrial structure of Inner Mongolia, Shanxi and Ningxia, which is

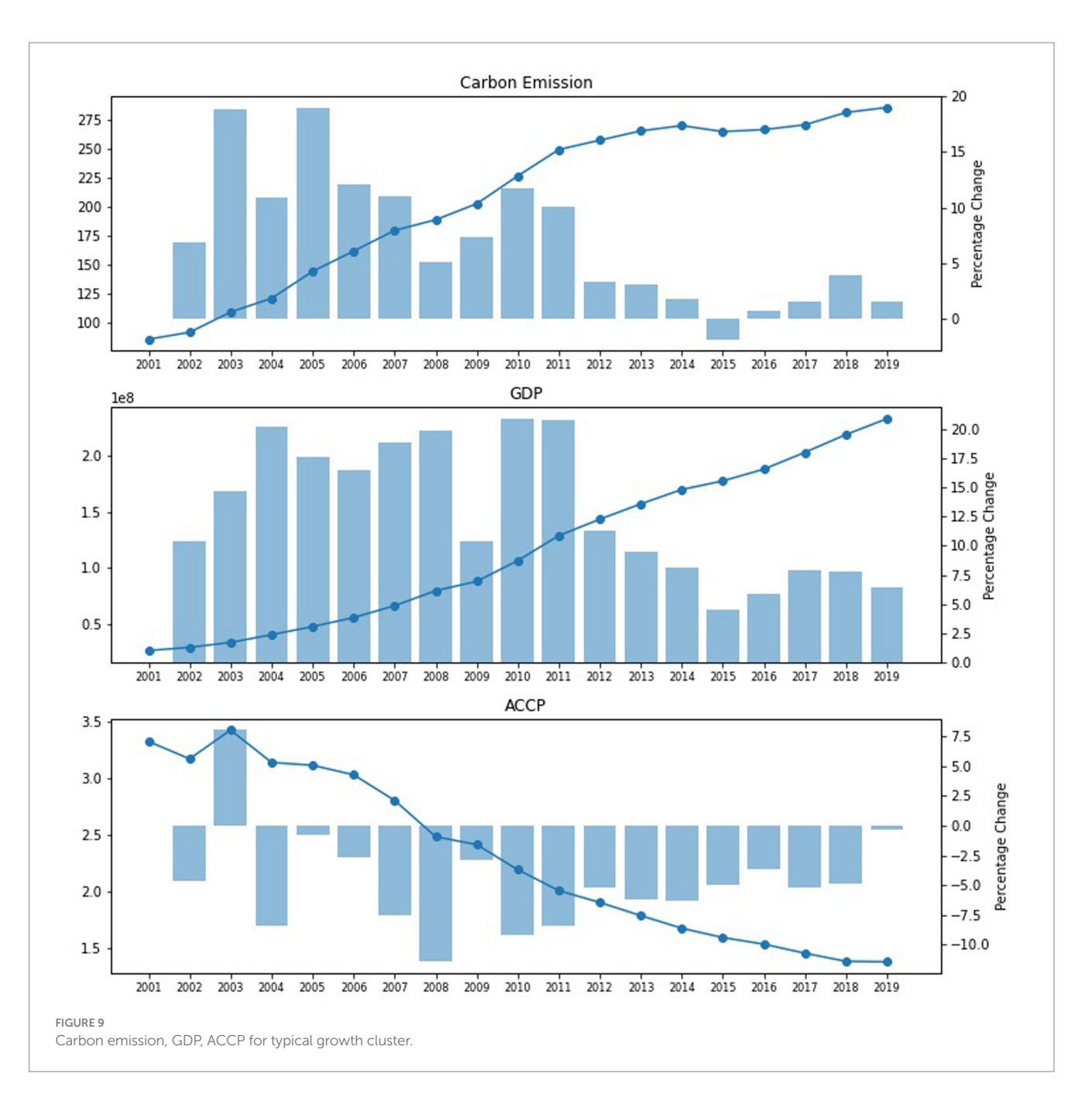


dominated by industries that highly rely on natural resources such as coal, oil and gas. Due to the nature of resource-based industries, energy plays an important role in their economic activities, and higher energy consumption is usually closely associated with increase in carbon emissions. These energy-intensive industries are accompanied by high carbon emissions during extraction, processing and utilization. Furthermore, the industrial structure of these regions is highly homogeneous leading to the difficulties with industrial upgrading and transformation. In addition to the resource dominated industrial structure, the energy structure in these regions also has a huge impact on the carbon emission pathways. The energy structure of Inner Mongolia, Shanxi and

Ningxia favors fossil fuels, contributing to the higher carbonintensive component of their energy sources, thus further pushing up the level of carbon emissions (Figure 9).

3.3.4 CE structure clustering

From the proportions of carbon emissions for three industries, three clusters are obtained from the hierarchical cluster analysis. The first cluster represents the general Chinese provinces and regions containing 27 provincial regions. Beijing and Shanghai belong to the second cluster, and Hainan forms the third clusters by itself. We named the first cluster as Benchmark Cluster. It remains a relatively stable industrial structure throughout the years with a slight but consistent

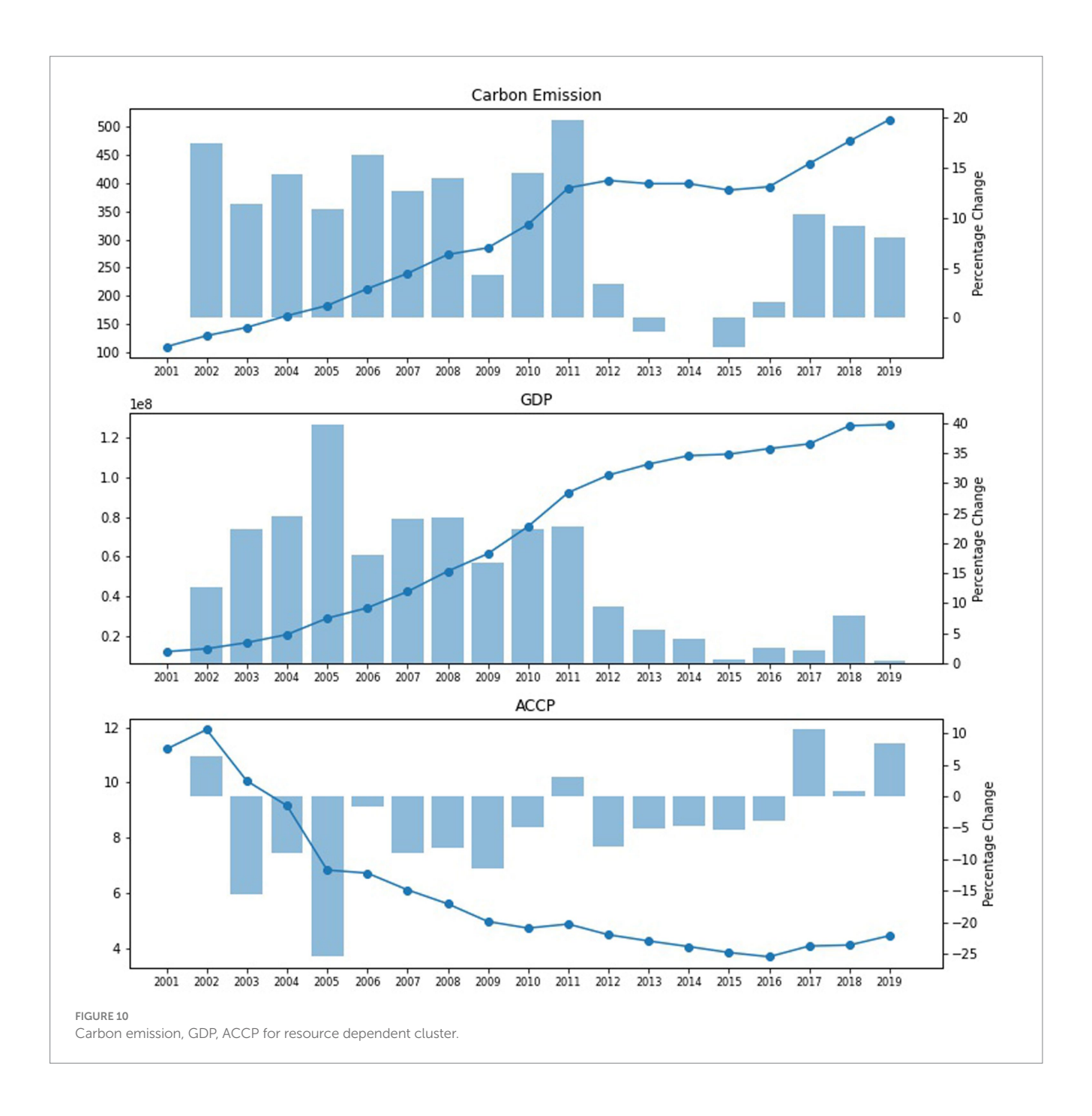


increase in the tertiary industry's proportion from 6.41% in 2001 to 8.07% in 2019, indicating a shift toward service-oriented economic activities. There is also a tiny increase from the secondary industry corresponding to the nation-wide industrialization development in the past two decades, while the first industry industry's weight drops from 7.77 to 4.03% over the study period. Benchmark Cluster gives a clear illustration about the patterns of Chinese industrial structure with respect to carbon emission and also can be viewed as a perfect standard for comparing the structural shifts for the other two clusters. The second cluster, named as Service- Booming Cluster, exhibits a clear transition characterized by significant decline in the primary industry, which is replaced by remarkable growth in the tertiary industry. The third cluster shows a very unique pattern of shrinking proportions in the tertiary industry as well as the first industry. We name it as Strategic-Transition Cluster after a deep analysis of the driven forces

behind its industrial structure change. Detailed investigation and discussion on these innovative phenomenons observed in the following sections (Figure 10).

4 Discussion

Based on provincial panel data from China (1996–2019), this study systematically explores the spatiotemporal patterns, driving mechanisms, and regional heterogeneity of carbon dioxide emissions using spatiotemporal geographically weighted regression (GTWR/SGTWR), spatial autocorrelation analysis, and clustering methods. The analysis reveals significant spatial aggregation and periodic evolution characteristics in China's carbon emissions, with pronounced regional differences in how driving factors influence



emissions. By constructing the TCE-GDP-ACCP clustering model, we classify provincial regions into four distinct development clusters, providing a scientific foundation for differentiated emission reduction policies.

4.1 Spatial and temporal dynamic characteristics of carbon emissions

In this study, the dynamic characteristic of urban-scale building CO_2 emissions in China was investigated through the calculation of total, food, water, live, traffic, energy and other and the population. Global Moran's I analysis confirms significant positive spatial autocorrelation (I > 0, p < 0.05), with eastern coastal provinces (e.g.,

Shandong, Jiangsu) forming "high-high" clusters due to concentrated energy-intensive industries and urban sprawl, while western regions (e.g., Qinghai, Tibet) displayed "low-low" aggregation (Zhang et al., 2025; Liu and Lv, 2024; Liu et al., 2024; Dong et al., 2024). Sectoral disparities further highlight spatial heterogeneity: residential and transportation emissions dominate urban hubs (e.g., Beijing-Tianjin-Hebei, Yangtze River Delta), correlating strongly with population density and private vehicle proliferation (9.3% annual growth) (Wang et al., 2023). Conversely, agricultural emissions cluster in the North China Plain, linked to intensive farming practices, whereas energy-dependent northern provinces (e.g., Shanxi) face elevated residential emissions from coal-reliant heating systems. These patterns emphasized the coupling between urbanization and carbon intensity, underscoring the need for spatially differentiated policies to address

sectoral and regional imbalances. Notably, in key Chinese metropolises like Beijing, Shanghai, Guangzhou, and Shenzhen, building CO2 emission growth remained comparatively low (Jia et al., 2025; Li et al., 2025; Zhou et al., 2024). In contrast, surrounding regions showed faster growth in building CO₂ emissions. Several factors explain the lower emission growth rates observed in highly developed cities: Firstly, economic growth in these cities has stabilized at high levels, and urbanization is already advanced, naturally limiting the expansion of energy demand. Secondly, these cities have likely implemented comprehensive emission reduction policies and technical measures, such as developing the renewable energy sector, which effectively curb the rise in CO₂ emissions (Zhang et al., 2020). In our study, China's carbon emissions exhibited distinct spatiotemporal heterogeneity during 1996-2019, characterized by four evolutionary phases (Section 3.1.2). The surge during 2000-2007 (12.17%/yr) aligns with rapid industrialization and urbanization, while the post-2013 decline (-1.77%/yr) directly reflects the efficacy of policy interventions such as the Air Pollution Prevention and Control Action Plan (2013) and renewable energy investments. Spatial autocorrelation analysis (Table 2) revealed weakening aggregation patterns after 2015 (Moran's I shifting from positive to negative), indicating increasing regional divergence in emission trajectories. This decentralization underscores the need for region-specific governance frameworks, as high-emission clusters (e.g., Inner Mongolia, Shanxi) persisted due to fossil fuel dependency, while coastal provinces (e.g., Jiangsu, Guangdong) demonstrated economic growth with moderated emissions through industrial upgrading.

4.2 Sectoral drivers and heterogeneous responses

Energy and transport sectors dominated post-2008 emissions highlighted structural challenges in decarbonizing heavy industry and mobility infrastructure. Conversely, food/water emissions declined post-2012, attributed to precision agriculture, wastewater treatment

TABLE 6 Variable definitions.

| Variable | Definition | Unit | Source |
|---------------------|--|--|---|
| TCE | Total Carbon Emissions | Mt CO ₂ | CEADs (2023) |
| ACCP | Avg. Carbon Cost of Production | tCO ₂ /10 ⁴ CNY GDP | Calculated (GDP/TCE) |
| GDP | Gross Domestic Product | 10 ⁴ CNY | China Statistical Yearbook |
| Food Emissions | CO ₂ from agricultural production | Mt CO ₂ | IPCC Guidelines (2001–2020) |
| Energy Emissions | CO ₂ from fossil fuel combustion | Mt CO ₂ | China Energy Statistical Yearbook |
| Moran's I | Spatial autocorrelation index | Dimensionless | Calculated via ArcGis |

technologies, and rising environmental awareness (Liu et al., 2024). This divergence exemplified a critical insight: While energy/transport require systemic transitions (e.g., grid decarbonization, electrification), food/water sectors offer a model for rapid mitigation via innovation and behavioral change. Spatiotemporal regression (GTWR/SGTWR) further quantified regional heterogeneity (Tables 6, 2): Northern China showed higher carbon intensity linked to coal-reliant heating and energy-intensive industries (e.g., ACCP = $4.45 \text{ tCO}_2/10^4 \text{ CNY}$ GDP in Shanxi). Eastern coastal cities (e.g., Shanghai) achieved emission decoupling through service-sector dominance (>80% tertiary industry) and clean energy adoption. Western regions exhibited lower emissions but faced ecological constraints (e.g., riverine CO₂ fluxes), necessitating nature-based solutions (Han et al., 2024).

4.3 Regional clustering and emission reduction path

Provincial emission trajectories are profoundly shaped by energy mix and industrial restructuring. Resource-dependent regions (e.g., Shanxi, Inner Mongolia), where coal dominates (>70% of energy consumption), exhibit the highest carbon intensity (ACCP = 4.45 tCO₂/10⁴ CNY GDP in 2019) and sluggish post-policy mitigation $(\Delta TCE = 3.54\%, 2012-2019)$, reflecting structural inertia in fossil fuel-reliant economies (Chen and Lu, 2023). In contrast, low-carbon exemplars (e.g., Beijing, Shanghai) achieved emission decoupling $(\Delta TCE = -0.06\%)$ through service-sector expansion (>80% tertiary industry) and clean energy adoption (>14% non-fossil share), validating the efficacy of "service-led decarbonization" strategies (Xiang et al., 2024; Wu and Zhang, 2024). However, typical growth provinces (e.g., Anhui, Heilongjiang) struggle with industrial path dependency, as secondary industries (>45% GDP share) and slow ACCP declines (-4.6% annually) sustain emission growth ($\Delta TCE = 1.73\%$) (Wang et al., 2018). These findings echo Wang, who stressed the role of energy transitions in breaking carbon lock-ins, advocating for renewable integration in coal-dependent regions and green financing to accelerate digital-industrial transitions in emerging economies. Such tailored approaches are critical to aligning regional pathways with China's "dual carbon" goals (Zan et al., 2024). Based on cluster-specific traits, we propose actionable policies: Resource-Dependent (e.g., Shanxi): Deploy CCUS in coal plants; hybrid wind-PV-hydrogen infrastructures. Ecological compensation for mining areas (e.g., Inner Mongolia's grassland restoration). Rapid Growth (e.g., Guangdong): Mandate renewable corridors (solar highways); green bonds for industrial park retrofits. Carbon tax pilot for highemission export industries. Low-Carbon Exemplar (e.g., Shanghai): Scale carbon trading to households; EV subsidies via tax credits. Export "smart city" decarbonization models to ASEAN. Typical Growth (e.g., Anhui): Biomass co-firing subsidies for coal plants; skills training for green jobs.

This study reveals the evolution path of carbon emissions in four provinces through spatial clustering (Table 7). This typology underscores the spatial and structural heterogeneity of emission pathways, where rapidly industrializing provinces (e.g., Jiangsu, Guangdong) require prioritized investments in smart grids and renewable energy integration to decouple economic growth from carbon intensity, while resource-dependent regions (e.g., Shanxi,

TABLE 7 Policy recommendations.

| Cluster | Policy recommendations |
|---------------------|--|
| Resource-dependent | Deploy CCUS in Shanxi's coal plants; diversify to wind/solar-hydrogen hybrids in Inner Mongolia |
| Rapid growth | Mandate renewable corridors in Jiangsu/ Guangdong; green infrastructure bonds for industrial parks |
| Low-carbon exemplar | Scale carbon trading in Beijing/Shanghai; incentivize public EV adoption via tax credits |
| Typical growth | Subsidize biomass retrofits in Anhui; green financing for Heilongjiang's heavy industry |

Inner Mongolia) demand accelerated transitions to clean energy systems, such as CCUS and hybrid wind-PV-hydrogen infrastructures (Sikarwar et al., 2024; Song et al., 2019). Resource-dependent provinces can establish a "coal-new energy" hybrid power generation system, and support a carbon market trading mechanism; low-emission demonstration areas can further promote the carbon inclusive system and encourage public participation. Low-carbon exemplars (e.g., Beijing, Shanghai) exemplify the efficacy of servicesector dominance and policy-driven innovation, yet their success highlights the need for scaling carbon-inclusive mechanisms to incentivize public participation in broader regions (Lou et al., 2014). Meanwhile, typical growth clusters face structural inertia, necessitating green financing to overcome industrial lock-ins and adopt biomass solutions (Gopikrishnan and Kuttippurath, 2025; Liu et al., 2025). Different regions face different challenges in policy implementation: the eastern region has obvious advantages in capital and technology, but the marginal cost of emission reduction is rising; the western region needs to overcome the problems of insufficient funds and shortage of technical personnel. It is recommended to support its low-carbon transformation through cross-regional cooperation and transfer payment mechanisms. By aligning policies with clusterspecific challenges and opportunities, this model not only enhances the precision of urban decarbonization but also advances China's dual carbon goals through spatially adaptive governance, balancing economic resilience with emission reduction imperatives.

5 Limitations and future directions

While this study provides a comprehensive analysis of China's provincial CO₂ emissions, several limitations warrant acknowledgment. First, data constraints (exclusion of Tibet, Hong Kong, and Macao due to missing data) may affect the completeness of spatial patterns. Second, the reliance on production-based accounting omits embodied carbon in interprovincial trade and consumption, potentially underestimating emissions in highly industrialized or consumer regions. Third, the clustering methodology, though robust, captures trajectories only up to 2019; post-pandemic economic shifts and recent policy accelerations (e.g., renewable energy investments post-2020) necessitate temporal extensions. Finally, the GTWR/SGTWR models, while accounting for spatiotemporal heterogeneity, do not fully integrate micro-scale urban dynamics (e.g., building-level

energy use) or behavioral factors influencing residential/transport emissions. Future research should: Adopt consumption-based accounting to quantify cross-regional carbon flows and allocate emission responsibilities more equitably. Develop integrated assessment models coupling socioeconomic scenarios (e.g., population aging, green tech diffusion) with climate targets. Explore technological pathways (e.g., hydrogen adoption in Resource-Dependent clusters) via techno-economic optimization. Addressing these gaps will enhance the granularity of regional decarbonization strategies and better align China's "dual carbon" goals with global climate governance frameworks.

6 Conclusion

This study pioneers a DTW-AHC-GTWR framework to decode China's provincial carbon trajectories. Key advances: (1) Dynamic clustering: Identified four emission clusters via ACCP-augmented paths, overcoming static K-means limitations. (2) Spatio-temporal tipping point: Empirically validated 2015 as Moran's I transition year (positive -> negative), demanding region-specific governance. (3) Sectoral decoupling evidence: Tech-driven declines in food/water emissions post-2016 contrast energy/transport inertia, offering rapid mitigation templates. Policy integration leverages these insights: (1) Resource-Dependent clusters prioritize CCUS-infrastructure hybrids. (2) Rapid Growth zones embed renewables in urban planning. (3) Limitations (e.g., Tibet data gaps) guide future remote-sensing validation. This reframes 'dual carbon' policies beyond aggregate targets, prioritizing spatial diversification through carbon-efficient pathways. Only by formulating corresponding strategies based on the characteristics and trends of each city can we effectively drive carbon peak actions at the city level and contribute to the nationwide carbon neutrality goals.

Data availability statement

The original contributions presented in the study are included in the article/supplementary material, further inquiries can be directed to the corresponding authors.

Author contributions

XC: Validation, Data curation, Writing – original draft, Methodology. SZ: Investigation, Writing – original draft, Visualization, Methodology. JL: Writing – original draft, Investigation, Data curation. JT: Funding acquisition, Writing – review & editing, Supervision. XM: Conceptualization, Writing – review & editing, Methodology, Supervision.

Funding

The author(s) declare that financial support was received for the research and/or publication of this article. The work was supported by Xi 'an Academy of Social Sciences General Project 25ZL26.

Conflict of interest

The authors declare that the research was conducted in the absence of any commercial or financial relationships that could be construed as a potential conflict of interest.

Generative AI statement

The authors declare that no Gen AI was used in the creation of this manuscript.

Any alternative text (alt text) provided alongside figures in this article has been generated by Frontiers with the support of artificial

References

CEADs. (2023). Carbon emission accounts&datasets for emerging economies. Available online at: https://www.ceads.net/.

Chen, H. L., and Lu, C. M. (2023). Research on the spatial effect and threshold characteristics of new-type urbanization on carbon emissions in China's construction industry. *Sustainability* 15:15825. doi: 10.3390/SU152215825

Chen, J. D., Xu, C., Li, K., and Song, M. L. (2018). A gravity model and exploratory spatial data analysis of prefecture-scale pollutant and CO₂ emissions in China. *Ecol. Indic.* 90, 554–563. doi: 10.1016/j.ecolind.2018.03.057

Companies and Markets. (2008). China Energy Statistical Yearbook, 2007. M2 Presswire.

Dong, M. F., Wang, G., and Han, X. F. (2024). Impacts of artificial intelligence on carbon emissions in China: in terms of artificial intelligence type and regional differences. *Sustain. Cit. Soc.* 113:105682. doi: 10.1016/J.SCS.2024.105682

Gopikrishnan, S. G., and Kuttippurath, J. (2025). Impact of the National Clean Air Programme (NCAP) on the particulate matter pollution and associated reduction in human mortalities in Indian cities. *Sci. Total Environ.* 968:178787. doi: 10.1016/J.SCITOTENV.2025.178787

Hair, J. F., Black, W. C., Babin, B. J., and Anderson, R. E. (2010). *Multivariate data analysis*. (7th ed.). Prentice Hall.

Han, J. Y., Qu, J. S., Maraseni, N. T., Zeng, J. J., Wang, D., Ge, Y. J., et al. (2024). Spatiotemporal analysis of the food-related carbon emissions of China: regional heterogeneity and the urban-rural divide. *J. Environ. Manag.* 370:122441. doi: 10.1016/J.JENVMAN.2024.122441

He, Y., Xing, Y. T., Zeng, X. C., Ji, Y. J., Hou, H. M., Zhang, Y., et al. (2022). Factors influencing carbon emissions from China's electricity industry: analysis using the combination of LMDI and K-means clustering. *Environ. Impact Assess. Rev.* 93:106724. doi: 10.1016/J.EIAR.2021.106724

 $IPCC.\ (2021).\ Emission\ factor\ database.\ Available\ online\ at:\ https://www.ipcc-nggip.iges.or.jp/EFDB/main.Php.$

Jia, H., Li, W. D., and Tian, R. T. (2025). Spatio-temporal influencing factors of the coupling coordination degree between China's new-type urbanization and transportation carbon emission efficiency. *Land* 14:623. doi: 10.3390/land14030623

Jiang, J. J., Ye, B., Xie, D. J., and Tang, J. (2017). Provincial-level carbon emission drivers and emission reduction strategies in China: combining multi-layer LMDI decomposition with hierarchical clustering. *J. Clean. Prod.* 169, 178–190. doi: 10.1016/j.jclepro.2017.03.189

Jiang, J. K., Zhu, S. L., Wang, W. H., Li, Y., and Li, N. (2022). Coupling coordination between new urbanisation and carbon emissions in China. *Sci. Total Environ.* 850:158076. doi: 10.1016/J.SCITOTENV.2022.158076

Li, W., Ji, Z., and Dong, F. (2022). Spatio-temporal analysis of decoupling and spatial clustering decomposition of CO2 emissions in 335 Chinese cities. *Sustain. Cities Soc.* 86:104156. doi: 10.1016/j.scs.2022.104156

Li, H., Wu, Q., Zhao, X., and Ma, L. (2024). The impact of digital economy on energy-related carbon emissions: evidence from Chinese provinces. *Energy* 290:132034. doi: 10.1016/j.Energy.2024.132034

Li, X. M., Zhou, X. Q., Zhao, Y. F., and Zhou, S. W. (2025). Exploring coupling coordination of new urbanization, green innovation and low-carbon development systems in China. *J. Clean. Prod.* 495:145022. doi: 10.1016/J.JCLEPRO.2025.145022

Liang, X. Y., Min, F., Huang, X. F., Cai, C., Zhou, L. L., and Wang, Y. Z. (2024). Spatial distributed characteristics of carbon dioxide emissions based on fossil energy consumption and their driving factors at provincial scale in China. *Energy* 309:133062-133062. doi: 10.1016/J.ENERGY.2024.133062

intelligence and reasonable efforts have been made to ensure accuracy, including review by the authors wherever possible. If you identify any issues, please contact us.

Publisher's note

All claims expressed in this article are solely those of the authors and do not necessarily represent those of their affiliated organizations, or those of the publisher, the editors and the reviewers. Any product that may be evaluated in this article, or claim that may be made by its manufacturer, is not guaranteed or endorsed by the publisher.

Lim, J. B., Kang, M. Y., and Jung, C. M. (2019). Effect of national-level spatial distribution of cities on national transport CO_2 emissions. *Environ. Impact Assess.* 77:162. doi: 10.1016/j.enpol.2018.05.037

Liu, B. J., Liu, R. B., and Lee, C. C. (2024). Efficiency evaluation of China's transportation system considering carbon emissions: evidence from big data analytics methods. *Total Environ.* 922:171031. doi: 10.1016/J.SCITOTENV.2024.171031

Liu, B., and Lv, J. H. (2024). Spatiotemporal evolution and tapio decoupling analysis of energy-related carbon emissions using nighttime light data: a quantitative case study at the city scale in Northeast China. *Energies* 17:4795. doi: 10.3390/EN17194795

Liu, Y. S., Yan, B., and Zhou, Y. (2015). Urbanization, economic growth, and carbon dioxide emissions in China: a panel cointegration and causality analysis. *J. Geogr. Sci.* 26, 131–152. doi: 10.1007/s11442-016-1259-2

Liu, M. L., Zhao, Q. H., Lang, Z. K., Du, X. P., and Wu, J. T. (2025). An integrated assessment system for regional carbon emissions: insights into China's sustainable development. *Energy* 317:134693. doi: 10.1016/J.ENERGY.2025.134693

Lou, L. P., Cheng, G. H., Deng, J. Y., Sun, M. Y., Chen, H. Y., Yang, Q., et al. (2014). Mechanism of and relation between the sorption and desorption of nonylphenol on black carbon-inclusive sediment. *Environ. Pollu.* 190, 101–108. doi: 10.1016/j.envpol.2014.03.027

Meng, G. F., Guo, Z., and Li, J. L. (2021). The dynamic linkage among urbanisation, industrialisation and carbon emissions in China: insights from spatiotemporal effect. *Sci. Total Environ.* 760:144042. doi: 10.1016/J.SCITOTENV.2020.144042

Qin, H. T., Huang, Q. H., Zhang, Z. Z., Lu, Y., Li, M. C., Xu, L., et al. (2019). Carbon dioxide emission driving factors analysis and policy implications of Chinese cities: combining geographically weighted regression with two-step cluster. *Sci. Total Environ.* 684, 413–424. doi: 10.1016/j.scitotenv.2019.05.352

Raymond, P. A., Hartmann, J., Lauerwald, R., Sobek, S., McDonald, C., Hoover, M., et al. (2013). Global carbon dioxide emissions from inland waters. *Nature* 503, 355–359. doi: 10.1038/nature12760

Research and Markets. (2008). Introducing the China Energy Statistical Yearbook, 2007. Edited by the Department together with Energy Bureau of National Development and Reform Commission or NDRC. *M2 Presswire*.

Sabbir, A. R. (1998). Efficient interactive agglomerative hierarchical clustering algorithm for hyperspectral image processing. United Kingdom: Raytheon optical systems, Inc.

Salvador, S., and Chan, P. (2007). Toward accurate dynamic time warping in linear time and space. *Intell. Data Anal.* 11, 561–580. doi: 10.3233/IDA-2007-11508

Sheng, P. F., and Guo, X. H. (2016). The long-run and short-run impacts of urbanization on carbon dioxide emissions. *Econ. Model.* 53, 208–215. doi: 10.1016/j.econmod.2015.12.006

Sikarwar, V. S., Mašláni, A., Van, O. G., Fathi, J., Hlína, M., Mates, T., et al. (2024). Integration of thermal plasma with CCUS to valorize sewage sludge. *Energy* 288:129896. doi: 10.1016/J.ENERGY.2023.129896

Song, C. F., Liu, Q. L., Qi, Y., Chen, G. Y., Song, Y. J., Yasuki, K., et al. (2019). Absorption-microalgae hybrid $\rm CO_2$ capture and biotransformation strategy—a review. *Inter. J. Green. Gas Con.* 88, 109–117. doi: 10.1016/j.ijggc.2019.06.002

Song, C., and Wang, G. (2021). Land carbon sink of the Tibetan plateau may be overestimated without accounting for the aquatic carbon export. *Proc. Natl. Acad. Sci.* 118:e2114694118. doi: 10.1073/pnas.2114694118

Song, Q. S., Zhou, N., Liu, T. L., Siehr, S. A., and Qi, Y. (2018). Investigation of a "coupling model" of coordination between low-carbon development and urbanization in China. *Energy Policy* 121, 346–354. doi: 10.1016/j.eiar.2019.04.006

Wang, L., and Chen, X. (2025). Policy-driven carbon emission reduction pathways in China's industrial parks: a multi-scale analysis. *J. Environ. Manag.* 351:124609. doi: 10.1016/j.jenvman.2025.124609

- Wang, Y. N., Chen, W., Kang, Y. Q., Li, W., and Guol, F. (2018). Spatial correlation of factors affecting CO2 emission at provincial level in China: a geographically weighted regression approach. *J. Clean. Prod.* 184, 929–937. doi: 10.1016/j.jclepro.2018.03.002
- Wang, L. Z., Sun, Y. X., and Xv, D. Y. (2023). Study on the spatial characteristics of the digital economy on urban carbon emissions. *Environ. Sci. Pollut. Res.* 30, 80261-80278. doi: 10.1007/S11356-023-28118-3
- Wei, L. Y., and Liu, Z. (2022). Spatial heterogeneity of demographic structure effects on urban carbon emissions. *Environ. Impact Assess. Rev.* 95:106790. doi: 10.1016/J.EIAR.2022.106790
- Wen, J. H., Huang, T. B., Cui, X. H., Zhang, Y. L., Shi, J. F., Jiang, Y. J., et al. (2024). Enhancing image alignment in time-lapse-ground-penetrating radar through dynamic time warping. *Remote Sens* 16:1040. doi: 10.3390/R\$16061040
- Wu, K. Y., Sun, C. Y., Zhang, J. Y., and Duan, J. H. (2023). Carbon neutrality along the global value chain: an international embedded carbon network analysis. *Environ. Sci. Pollut. Res.* 30, 122051–122065. doi: 10.1007/S11356-023-30680-9
- Wu, S. S., Wang, Z. Y., Du, Z. H., Huang, B., Zhang, F., and Liu, R. Y. (2021). Geographically and temporally neural network weighted regression for modeling spatiotemporal non-stationary relationships. *Int. J Geoer. Inf.* 35, 582–608. doi: 10.1080/13658816.2020.1775836
- Wu, Y. F., and Zhang, Q. (2024). The confrontation and symbiosis of green and development: coupling coordination analysis between carbon emissions and spatial development in urban agglomerations of China. *Sustain. Cities Soc.* 106:105391. doi: 10.1016/J.SCS.2024.105391
- Xiang, W. X., Lan, Y. Q., Gan, L., and Li, J. (2024). How does new urbanization affect urban carbon emissions? Evidence based on spatial spillover effects and mechanism tests. *Urb. Clim.* 56:102060. doi: 10.1016/J.UCLIM.2024.102060

- Xu, X. (2019). The slowdown of China's economic growth in terms of statistics. Front. Econ. Chi. 14, 72–79. doi: 10.3868/s060-008-019-0005-5
- Yang, S. D., Yang, X., Gao, X., and Zhang, J. X. (2022). Spatial and temporal distribution characteristics of carbon emissions and their drivers in shrinking cities in China: empirical evidence based on the NPP/VIIRS nighttime lighting index. *J. Environ. Manag.* 322:116082. doi: 10.1016/J.JENVMAN.2022.116082
- Yao, F., Zhu, H. X., and Wang, M. J. (2021). The impact of multiple dimensions of urbanization on CO₂ emissions: a spatial and threshold analysis of panel data on China's prefecture-level cities. *Sustain. Cities Soc.* 73:103113. doi: 10.1016/j.scs.2021.103113
- Zan, X. Z., Ji, P. J., Ying, Y. X., Jiang, L., Lin, X. Q., Wu, A. J., et al. (2024). Offshore carbon storage from power plants based on real option and multi-period source-sink matching: a case study in the eastern coastal China. *Car. Cap. Sci. Tech.* 13:100314. doi: 10.1016/J.CCST.2024.100314
- Zhang, F., Deng, X. Z., Phillips, F., Fang, C. L., and Wang, C. (2020). Impacts of industrial structure and technical progress on carbon emission intensity: evidence from 281 cities in China. *Tech. For. Soc. Chang.* 154:119949. doi: 10.1016/j.techfore.2020.119949
- Zhang, Y., Liu, R., Wang, Y., and Chen, J. (2023). Regional disparities and driving factors of $\rm CO_2$ emissions in China's residential sector: a spatial-temporal analysis. *Sci. Total Environ.* 876:163032. doi: 10.1016/j.scitotenv.2023.163032
- Zhang, Z., Wang, Z., Zong, J., Zhang, H. J., Hu, Y. F., Xiao, Y. L., et al. (2025). Spatial and temporal changes and influencing factors of mercury in urban agglomeration land patterns: a case from Changchun area, old industrial base of Northeast China. *Land* 14:652. doi: 10.3390/LAND14030652
- Zhang, C. G., and Zhao, W. (2024). Panel estimation for income inequality and CO 2 emissions: a regional analysis in China. *Appl. Energy* 136, 382–392. doi: 10.1016/j.apenergy.2014.09.048
- Zhou, Y., Lin, H. M., Li, C. S., and Ding, L. Y. (2024). Spatio-temporal patterns and impact mechanisms of CO₂ emissions from China's construction industry under urbanization. *Sustain. Cit. Soc.* 106:105353. doi: 10.1016/J.SCS.2024.105353